Sensors and Actuators B 205 (2014) 199–205

Contents lists available at ScienceDirect

Sensors and Actuators B: Chemical

journal homepage: www.elsevier.com/locate/snb

Highly sensitive palladium oxide thin film extended gate FETs as pH sensor

Atanu Das [a], Danny Hsu Ko [a], Chia-Hsin Chen [a], Liann-Be Chang [a], Chao-Sung Lai [a], Fu-Chuan Chu [a], Lee Chow [b], Ray-Ming Lin [a,*]

[a] Department of Electronic Engineering and Green Technology Research Center, Chang Gung University, 259 Wen-Hwa 1st Road, Kwei-Shan, Taoyuan 33302, Taiwan
[b] Department of Physics, University of Central Florida, Orlando 32816, USA

ARTICLE INFO

Article history:
Received 13 May 2014
Received in revised form 19 August 2014
Accepted 19 August 2014
Available online 3 September 2014

Keywords:
EGFET
Palladium oxide
pH sensor
Super-Nernstian sensitivity

ABSTRACT

It is well-known that palladium readily absorbs hydrogen gas at room temperature. Based on this unique property of palladium, palladium oxide (PdO)-sensitive membrane in the extended gate field-effect transistor (EGFET) configurations have been evaluated as a detector for hydrogen ions in pH buffer solutions. The PdO thin film was prepared by a two-step process through reactive electron beam evaporation and subsequent thermal oxidation in an optimal O_2 flow. Our results indicate that the PdO-based EGFET sensor showed super-Nernstian sensitivity approximately 62.87 mV/pH, while exhibiting good linearity as well as good stability between pH 2 and pH 12. Our research demonstrates that PdO membrane can be used in EGFET structure without compromising sensitivity achieved by conventional methods. Furthermore, the disposable PdO sensor shows great potential for low cost biochemical detection due to its simplified fabrication and measurement system.

1. Introduction

The detection of ions and molecules in a biochemical environment plays a significant role in chemical science and biotechnological application. The basis of an ion-sensitive field-effect transistor (ISFET) is derived from a metal-oxide semiconductor field-effect transistor (MOSFET), of which the metal gate is hereby substituted by an ion-sensitive membrane with direct contact with a buffer solution [1]. Since the invention of the first ISFET by Bergveld in 1970 [2], various techniques and sensing membranes have been exploited. The potential of these solid-state devices have attracted a great deal of attention, due to their numerous advantages such as miniaturization, chip-circuit design and low cost in manufacturing. In particular, they are an excellent candidate for the integration of biochemical sensors in microelectronics. Several ISFET-based biochemical sensors have been proposed [3,4]. However, owing to the fragile nature of membrane degradation in extreme conditions, extended gate field-effect transistor (EGFET) configuration has been developed to prolong stable operation. The mechanism of surface ion adsorption in ISFET and EGFET are essentially the same, with the major difference that EGFET configuration can only be used in low impedance membranes. EGFET is a subset of the ISFET family line, which modifies the ISFET into a two-part design. The sensing membrane is immersed in the solution, while connected to a remote FET IC chip for real-time analysis [1,5,6]. This approach enables us to swap the sensing membrane from any chemical damage instead of fabricating a whole new device.

Prompted by the demand for low cost chemical sensors, researchers looked into SiO_2 initially for pH sensitive membrane. The search for a more compatible material continued as sensitivity and stability impacted the performance of these chips. Since the realization of Ta_2O_5 as a pH-sensing membrane in 1981 by Matsuo et al. [7], various research groups have demonstrated the use of different sensing membranes such as Al_2O_3 [8], Si_3N_4 [4], SnO_2 [9], Er_2O_3 [10], Si nanowire/SiO_2/Al_2O_3 [11], IrO_X [12], Gd_2O_3/SiO_2 stacked oxide [13], silicon nanowire [14], Ru-doped TiO_2 [15] film in order to enhance detection capabilities. As the Nernst limit of pH sensitivity is 59 mV/pH, "super-Nernstian" sensitivity >59 mV/pH could promise a far more precise detection in monitoring the pH levels in blood and extracellular fluids.

In the 1980s, both Grubb and King [16] and Liu et al. [17] demonstrated the use of palladium–palladium oxide as a wire form electrode for their sensor fabrication. Both fabricated sensors revealed merits in pH detection, with the exception reported by

* Corresponding author. Tel.: +886 3 2118800x5790; fax: +886 3 2118507.
E-mail address: rmlin@mail.cgu.edu.tw (R.-M. Lin).

http://dx.doi.org/10.1016/j.snb.2014.08.057
0925-4005/

Liu et al., for exceeding Nernstian behavior with 71.4 ± 5 mV/pH. Grubb and King employed high temperature thermal oxidation of the palladium wire, whereas Liu et al. used electrochemical anodization. This was followed by the works of Kinoshita et al. [18] and Bloor et al. [19], whose groups also fabricated Pd–PdO pH electrode via thermal oxidation and electrochemical route respectively. Then in 1986, Karagounis et al. [20] demonstrated the possibility of fabricating Pd–Pdo thin film potentiometric pH sensor through RF reactive sputtering technique, reaching a pH sensitivity of 54 mV/pH in the pH range between 3 and 9.

Despite the promising developments in biochemical sensors, Pd–PdO-based sensors in EGFET configurations have not yet been reported. Therefore in this investigation, we propose a highly sensitive membrane consisting of PdO thin film as a pH sensor in the EGFET format. The sensor's performances in sensitivity, stability and reversibility were measured and analyzed. The experimental results have demonstrated that super-Nernstian pH response was reached with similar sensitivities achieved by conventional methods. These findings demonstrate a novel and effective design of a biochemical sensor by unifying the compound semiconductor sensing membrane with the silicon integrated chip technology.

2. Experimental details

2.1. PdO film preparation

Extended gate field-effect transistors, comprised of PdO thin film sensing membranes were fabricated on sapphire substrate and encapsulated on a copper clad FR-4 printed circuit board (PCB) laminate sheet. To begin with, 130 nm thickness of palladium oxide film was deposited by reactive electron beam (E-Beam) evaporation from a 99.999% pure Pd slug on a two inch sapphire substrate under O_2 flow of 20 sccm. The PdO thin film on sapphire then underwent an annealing in furnace at 973 K for an hour in O_2 flow of 1 slm. The two-step process was employed for the enhanced formation of PdO film. Morphology analysis was done using field emission scanning electron microscopy (FE-SEM). In addition, X-ray photoelectron spectroscopy (XPS) study was employed to characterize palladium–oxygen species on the surface of PdO film. Analysis through Hall measurement revealed the p-type semiconductive nature of PdO film with sheet resistivity, sheet carrier concentration and mobility of about 1221 Ω/□, 5.93×10^{14} cm^{-2} and 8.61 cm^2 V^{-1} s^{-1} respectively.

2.2. PdO sensor chip fabrication

Copper Clad FR-4 – PCB laminate sheet was first etched to fabricate a mounting template for the sensor chip as shown in Fig. 1(a). Samples of 1×1 cm^2 size were scribed from the native wafer for sensor chip fabrication. For pH detection studies, 1×1 cm^2 PdO/sapphire sample was mounted on square shaped area and bonded via silver paste. Silver paste was then applied carefully in the surrounding edges of the PdO layer and extended to copper plate, as to form the conductive line between sensing membrane and PCB. A homemade epoxy package was employed to encapsulate sensor chip and copper line while exposing a sensing area of approximately 0.25 cm^2 free from epoxy. The completed sensor as shown in Fig. 1(b) chip was immersed in pH 7 buffer solution for 24 h, allowing sensing surface to stabilize prior to current–voltage (I–V) measurement. A Texas Instruments n-MOSFET CD4007UBE was used as the FET in the EGFET device. The dimension n-MOSFET used for our measurement consists of gate length and gate width of 10 μm and 30 μm, respectively. We have used signal line of coaxial cable to connect copper metal line of fabricated PdO sensor chip and the gate of n-MOSFET as shown in Fig. 1(c). Fig. 1(d) shows the schematic diagram of completed PdO pH sensor chip.

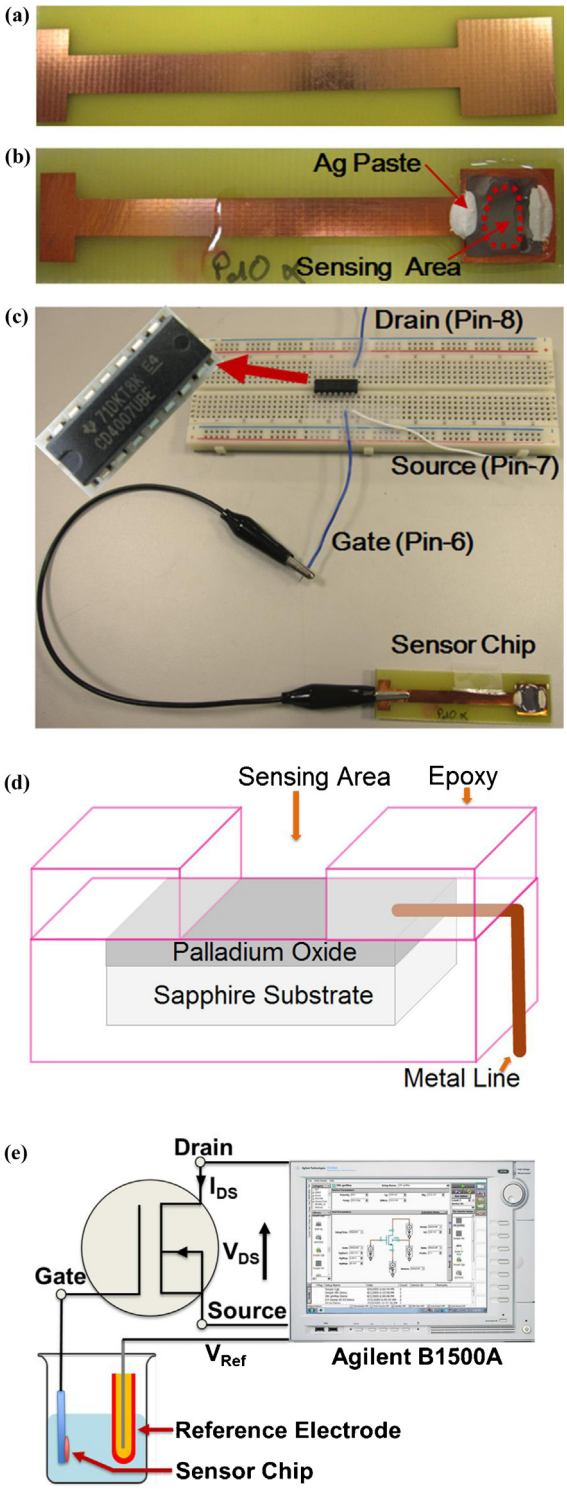

Fig. 1. Photograph of (a) bare PCB mounting template, (b) encapsulated PdO sensor chip and (c) final PdO sensor chip connected to the gate of n-MOSFET; schematic illustration of the (d) fabricated PdO sensor chip and (e) I–V measurement setup for the PdO pH-EGFET sensor.

2.3. Measurement of sensor chip

All current–voltage measurements took place in a shielding box in order to prevent any light exposure or electromagnetic

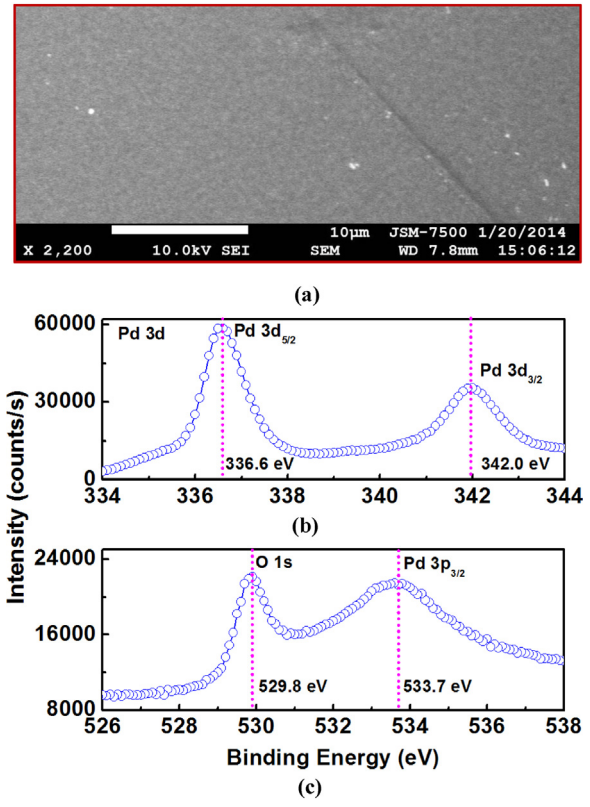

Fig. 2. (a) Surface morphology of PdO film by FE-SEM (×2.2 K). X-ray photoelectron spectra showing binding energy of (b) Pd $3d_{5/2}$, Pd $3d_{3/2}$ and (c) O 1s, Pd $3p_{5/2}$ core level electrons of PdO film.

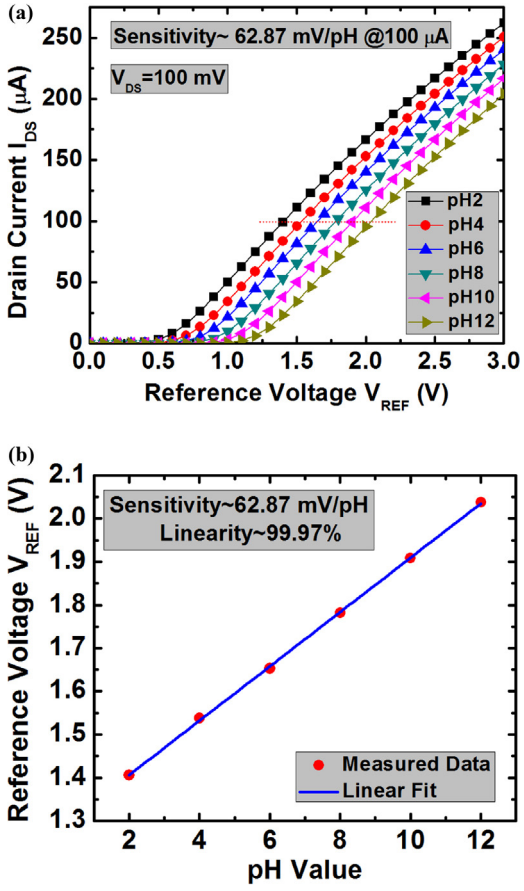

Fig. 3. (a) Transfer characteristics (I_{DS}–V_{REF}) for the PdO ion-sensitive EGFET sensor in the linear regime for different pH values from 2 to 12. (b) Linearity of PdO EGFET sensor in linear region.

interference. Variation in the solution temperature also can affect the sensor sensitivity as Nernst law is proportional to temperature. We have performed all the measurement of PdO sensor in room temperature (300 ± 2 K). Buffer solutions of pH 2, 4, 6, 8, 10 and 12 were obtained from Merck Chemicals. The pH-sensing properties in terms of sensitivity, linearity, hysteresis, drift were measured in various pH buffer solutions through Ag/AgCl reference electrode by Agilent B1500A semiconductor parameter analyzer. Fig. 1(e) shows the schematic diagram of the *I–V* measurement setup for PdO EGFET pH sensor.

3. Results and discussion

3.1. PdO film characterizations

Fig. 2(a) shows the top-view FE-SEM images of the surface morphology of PdO film, which suggests a relatively smooth surface of the film. The XPS spectrum of PdO film is presented in Fig. 2(b) and (c). The Pd $3d_{5/2}$ and Pd $3d_{3/2}$ doublet binding energy situated at 336.6 eV and 342.0 eV (Fig. 2(b)) respectively corresponds to the chemical state of PdO. The binding energy peak of the O 1s situated at 529.8 eV and the Pd $3p_{5/2}$ signal situated at 533.7 eV (Fig. 2(c)) which also correspond to the chemical state of PdO. The binding energy peaks determined are in agreement with that previously reported values for palladium oxide [21]. Taken together, it is verified that the formation of PdO layer during the combined process of reactive EB deposition in O_2 flow and furnace annealing process in O_2 ambient.

Analysis on PdO membrane's pH sensitivity, linearity, real-time response, hysteresis and drift were examined in order to determine its sensing characteristics.

3.2. Sensitivity and linearity (linear region)

In accordance to the EGFET theory, the relationship between I_{DS} vs. V_{REF} in the linear region can be expressed as follows:

$$I_{DS} = \frac{W\mu_n C_{ox}}{2L}[2(V_{REF} - V_{T(EGFET)})V_{DS} - V_{DS}^2] \quad (1)$$

where W/L denotes the channel width to length ratio, μ_n denotes the electron mobility in the channel, C_{ox} denotes the gate capacitance per unit area, $V_{T(EGFET)}$ denotes the threshold voltage of EGFET sensor, V_{REF} and V_{DS} are the reference and the drain-source voltages. The $V_{T(EGFET)}$ could be expressed in the following formula [15],

$$V_{T(EGFET)} = V_{T(MOSFET)} - \frac{\Phi_M}{q} + E_{REF} + \chi^{Sol} - \phi \quad (2)$$

where the $V_{T(MOSFET)}$ is the threshold voltage of MOSFET, Φ_M is the work function of the metal gate (reference electrode) relative to the vacuum, E_{REF} is the potential of the reference electrode, χ^{Sol} is the surface dipole potential of the buffer solution, and φ is the surface potential at the electrolyte/sensing film interface.

The I_{DS}–V_{REF} characteristics are shown in Fig. 3(a) for PdO EGFET sensors in the linear region. The I_{DS}–V_{REF} curve in linear region shows a uniform shift of the threshold voltage to higher voltage with the decreasing concentration of the hydrogen ions, i.e., the threshold voltages shifts from the left to the right as the hydrogen ions concentration decreased. The pH sensitivity and linearity of the PdO film was derived from the I_{DS}–V_{REF} curves at I_{DS} = 100 µA in pH solutions ranging from pH 2 to pH 12 as shown in Fig. 3(b).

The pH voltage sensitivity and linearity can then be extracted as follows,

$$\text{pH voltage sensitivity} = \frac{V_{T(EGFET)}(x_2) - V_{T(EGFET)}(x_1)}{\text{pH}(x_2) - \text{pH}(x_1)} = \frac{\Delta V_{T(EGFET)}}{\Delta \text{pH}} \quad (3)$$

The sensitivity of the PdO EGFET sensor was calculated to be 62.87 mV/pH and linearity was revealed to be 99.97%. These results have demonstrated that the PdO sensing membrane exhibits a linear pH change. We have measured five different PdO sensor chip prepared in different batches. The sensitivity values in pH range from 2 to 12 are found to be 60.38, 60.43, 61.60, 62.87, 65.31 mV/pH. All of the sensor chips have shown sensitivity greater than 59 mV/pH. The average sensitivity is 62.11 mV/pH. The calculated standard deviation is 2.05. We have presented data from the sensor chip of sensitivity 62.87 mV/pH which is close to the calculated average sensitivity. Considering a maximum Nernst response of 59 mV/pH at 293 K, an error of 1 K leads to 0.2 mV/pH which results a variation of ±0.4 mV/pH in sensor output in room temperature (300 ± 2 K). Therefore, temperature effect on sensor output is within experimental error and negligible. In comparison, the super-Nernstian sensitivity achieved in our PdO EGFET sensor is higher than the previously reported sensitivity for PdO thin film [20]. Recently, super-Nernstian response was achieved through double gate MOSFET configuration [22,23]. The capacitive coupling between its bottom gate and top gate can be controlled so that any higher desired super-Nernstian sensitivity of over 59 mV/pH can be attained via a well optimized design of bottom gate and top gate. This certainly does not apply to our PdO EGEFT system, as we have opted for an easier configuration. Super-Nernstian response achieved in several reported articles, including our observation does not violate the concept of 'Nernst Law' or 'Site Binding Model for insulator-electrolyte interface', rather it is an exception of the 'Nernst Law' and 'Site Binding Model'. The super-Nernstian could be related to the enhanced proton-exchange process [24] due to the increased oxidation state of PdO metal-oxide. The difference in fabrication conditions lead to different oxidation states of the metal-oxide thin film as higher oxidation states resulted in higher sensitivity [25]. Ultimately we believe that the enhanced PdO formation through two-step oxidation (reactive E-beam and furnace annealing in optimal O_2 flow) could be responsible for the super-Nernstian pH response in our study.

3.3. Sensitivity and linearity (saturation region)

Saturation occurs when a channel has been created, allowing current to flow between the drain and source. With different amounts of H^+ ions accumulated on the surface in response to the pH buffer solution, saturation sensitivity and linearity can be derived from the I_{DS}–V_{DS} curves in buffer solutions ranging from pH 2 to pH 12. Fig. 4(a) demonstrated the I_{DS}–V_{DS} characteristics of PdO sensor in pH = 2 to 12 when MOSFET was operating in the saturation region at V_{REF} of 2 V. It shows that the I_{DS}–V_{DS} curve shifts downward with an increase in pH values. For the saturation region of the PdO EGFET, the I_{DS}–V_{DS} can be expressed as

$$I_{DS} = \frac{W\mu_n C_{ox}}{2L}[(V_{REF} - V_{T(EGFET)})^2] \quad (4)$$

The pH current sensitivity can be expressed as follows,

$$\text{pH current sensitivity} = \frac{\sqrt{I_{DS}}(y_2) - \sqrt{I_{DS}}(y_1)}{\text{pH}(y_2) - \text{pH}(y_1)} = \frac{\Delta\sqrt{I_{DS}}}{\Delta \text{pH}} \quad (5)$$

The derived pH current sensitivity was approximately 1.08 $(\mu A)^{1/2}$/pH which is also notably high, with a linearity of 99.92%

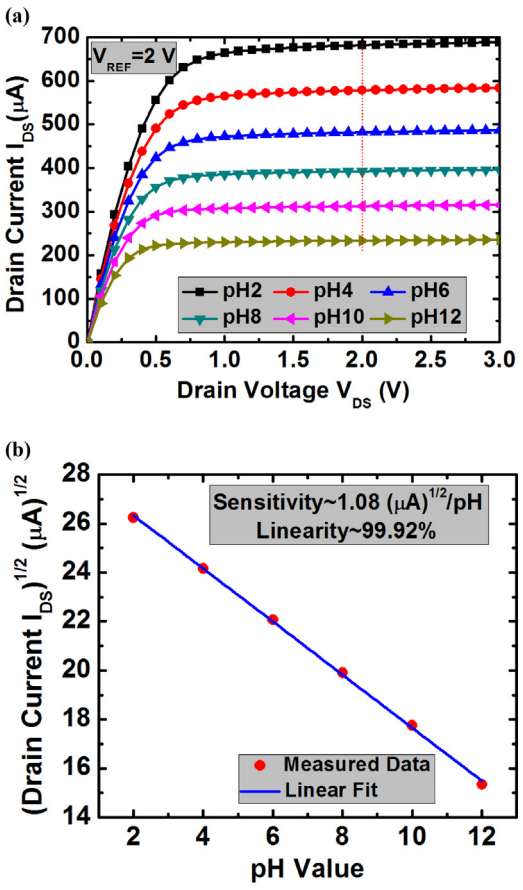

Fig. 4. Output characteristics (I_{DS}–V_{DS}) for the pH-EGFET sensors in the saturation regime for different pH values from 2 to 12. (b) Linearity of the I_{DS} of PdO EGFET sensor in saturation region.

as shown in Fig. 4(b). The result is an indication that $\sqrt{I_{DS}}$ linearly depends on the pH value in the saturation region.

3.4. Stability and reliability

Moreover, the stability of the device was investigated. For real-time response, we have used program in Agilent Easy Expert Software that monitored the drain current as a function of time, while keeping the drain bias (V_D) and gate bias (V_G) constant. Fig. 5 shows the real-time responses of I_{DS} for PdO sensor chip dipped

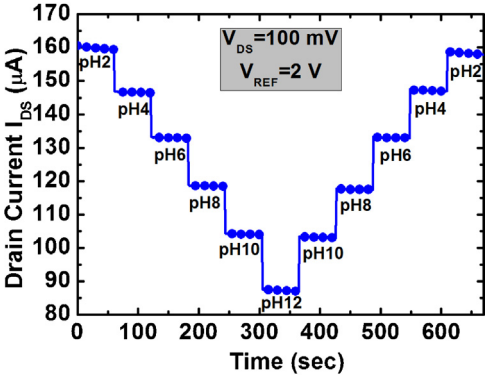

Fig. 5. Real-time I_{DS} responses of PdO sensor in a pH loop of 2 → 12 → 2 at V_{REF} of 2 V.

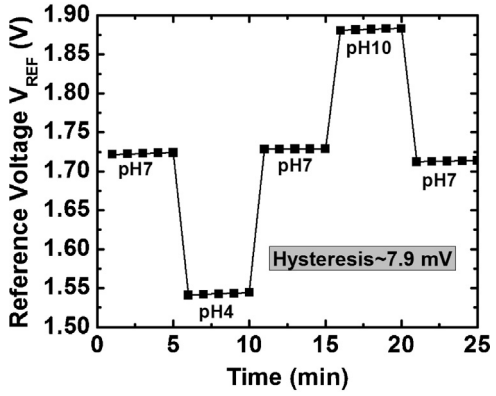

Fig. 6. Hysteresis characteristic of PdO sensor in a pH loop of 7 → 4 → 7 → 10 → 7 over a period of 25 min.

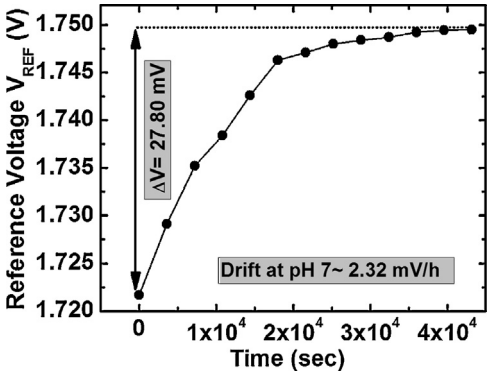

Fig. 7. Drift characteristic of PdO measured in pH 7 for 12 h.

for 60 s in each buffer solution of different pH values (pH loop: 2 → 12 → 2) at a V_{REF} of 2 V and V_{DS} = 100 mV. The cyclic step determines the accuracy of the sensor within a period of 660 s. It is a real-time exhibition of reliability, such that the I_{DS} decreases linearly as the pH value increases and vice versa. As shown in this figure, the fabricated PdO EGFET has exhibited almost perfect symmetric response together with low hysteresis due to the buffer solution variations.

Fig. 6 shows the hysteresis effect of the PdO sensing membrane. Hysteresis is known to be related to chemical interaction between ions in an electrolyte and slow reacting surface-sites underneath the membrane surface and/or the surface defects of the membrane [26]. For hysteresis characteristic, we have measured a family of I_D–V_G curves for each pH value when PdO sensing membrane was immersed in alternating cycles of pH buffer solutions i.e. pH 7 → pH 4 → pH 7 → pH 10 → pH 7 for 5 min in each pH buffer solution. Next, the reference bias voltage for a fixed drain current of 100 μA were extracted from each curve and plotted with different pH values. The net hysteresis was calculated as a difference between the initial reference voltage and final reference voltage at pH 7 to be 7.9 mV. In addition, drift in the reference voltage or threshold voltage of EGFET was studied for long-term reliability of electrochemical sensors which relates to OH^- adsorption on sensing film surface at different buffer solutions [27]. The potential drift phenomenon is common in ion selective pH sensors and the 3–10 mV drift is considered small [28]. In this work, the drift of the PdO sensor was measured in pH 7 buffer solution for 12 h. The drift property is compared by calculating the drift rate, ΔV_{REF}/h. For drift characteristic, we also measured a family of I_D–V_G curve in pH 7 for 12 h for long-term drift measurement. Similarly, the reference bias voltage for fixed drain current of 100 μA were extracted from each curve and plotted with time. Our PdO pH sensor drift was characterized by initial drift of 7.4 mV and long-term drift rate of 2.32 mV/h as shown in Fig. 7. As threshold voltage shifted toward positive direction during drift measurement, therefore it is believed that initial fast drift may be caused by OH^- ion adsorption in PdO sensing surface site and remaining lower long-term drift caused by slow diffusion of OH^- in slowly reacting buried site of PdO film. When compared to our result, lower drift of 0.38 mV/h and 0.3 ± 0.1 mV/h were achieved in ruthenium oxide [25] and iridium oxide [29] metal-oxide pH sensors. Nonetheless our PdO film has lower long-term drift rate compared to other reported result on SnO_2 [30], a-WO_3 [31] sensing membrane.

As the sensor suffers damage after being immersed in solution, from the experimental observation, we would like to mention that the PdO sensor chip we have fabricated has shown good sensing properties in terms of sensitivity and linearity for 6–7 complete cycles (pH 2 → pH 12 → pH 2) of measurements in the pH range from 2 to 12. After that sensitivity and linearity properties degrade with no such visual degradation on the PdO surface.

4. Conclusions

In this study, we have reintroduced the PdO thin film based sensor via EGFET technique. Top-view FE-SEM image has suggested a relatively smooth surface morphology of PdO film prepared through a two-step process. Material analysis with XPS confirmed the chemical state of PdO through Pd $3d_{5/2}$ and Pd $3d_{3/2}$ doublet, Pd $3p_{5/2}$ and O 1s binding energy peak positions. The fabricated PdO sensor seemed suitable for pH sensing, as super-Nernstian sensitivity of 62.87 ± 2 mV/pH, linearity of 99.97%, low hysteresis of 7.9 mV and drift rate of 2.32 mV/h were achieved. The sensitivity and linearity (both in linear and saturation regime), reversibility, hysteresis effect, and drift analysis have indicated the sensor chip to be reasonably accurate, stable and reliable in pH testing. As a result, the performance of a PdO-based sensor in EGFET configuration not only benefits disposability in replacing damaged sensing membranes, but also maintaining an adequate pH-sensing standard. Thus, palladium oxide based EGFET shows great promise in biochemical sensing applications.

Acknowledgement

This work was financially supported by the National Science Council (NSC), Taiwan currently known as Ministry of Science and Technology (MOST), under contract no. NSC-101-2221-E-182-047-MY2.

References

[1] J. van der spiegel, I. Lauks, P. Chan, D. Babic, The extended gate chemically sensitive field effect transistor as multi-species microprobe, Sens. Actuators (1983) 291–298.
[2] P. Bergveld, Development of an ion-sensitive solid-state device for neurophysiological measurements, IEEE Trans Biomed Eng BME-17 (1970) 70–71.
[3] P.V. Bobrov, Y.A. Tarantov, S. Krause, W. Moritz, Chemical sensitivity of an ISFET with Ta_2O_5 membrane in strong acid and alkaline solutions, Sens. Actuators B: Chem. 3 (1991) 75–81.
[4] M.N. Niu, X.F. Ding, Q.Y. Tong, Effect of two types of surface sites on the characteristics of Si_3N_4-gate pH-ISFETs, Sens. Actuators B: Chem. 37 (1996) 13–17.
[5] J.C. Chen, J.C. Chou, T.P. Sun, S.K. Hsiung, Portable urea biosensor based on the extended-gate field effect transistor, Sens. Actuators B: Chem. 91 (2003) 180–186.
[6] J.M. Rothberg, W. Hinz, T.M. Rearick, J. Schultz, W. Mileski, M. Davey, et al., An integrated semiconductor device enabling non-optical genome sequencing, Nature 475 (2011) 348–352.
[7] T. Matsuo, M. Esashi, Methods of ISFET fabrication, Sens. Actuators 1 (1981) 77–96.
[8] L. Bousse, H.H. van den Vlekkert, N.F. de Rooij, Hysteresis in Al_2O_3-gate ISFETs, Sens. Actuators B: Chem. 2 (1990) 103–110.

[9] Y.L. Chin, J.C. Chou, T.P. Sun, H.K. Liao, W.Y. Chung, S.K. Hsiung, A novel SnO_2/Al discrete gate ISFET pH sensor with CMOS standard process, Sens. Actuators B: Chem. 75 (2001) 36–42.
[10] T.M. Pan, J.C. Lin, M.H. Wu, C.S. Lai, Study of high-k Er_2O_3 thin layers as ISFET sensitive insulator surface for pH detection, Sens. Actuators B: Chem. 138 (2009) 619–624.
[11] O. Knopfmacher, A. Tarasov, W. Fu, M. Wipf, B. Niesen, M. Calame, et al., Nernst limit in dual-gated Si-nanowire FET sensors, Nano Lett. 10 (2010) 2268–2274.
[12] E. Prats-Alfonso, L. Abad, N. Casañ-Pastor, J. Gonzalo-Ruiz, E. Baldrich, Iridium oxide pH sensor for biomedical applications. Case urea-urease in real urine samples, Biosens. Bioelectron. 39 (2013) 163–169.
[13] L.B. Chang, H.H. Ko, Y.L. Lee, C.S. Lai, C.Y. Wang, The electrical and pH-sensitive characteristics of thermal $Gd_2O_3SiO_2$-stacked oxide capacitors, J. Electrochem. Soc. 153 (2006) G330–G332.
[14] Y. Cui, Q. Wei, H. Park, C.M. Lieber, Nanowire nanosensors for highly sensitive and selective detection of biological and chemical species, Science 293 (2001) 1289–1292.
[15] J.C. Chou, C.W. Chen, Fabrication and application of ruthenium-doped titanium dioxide films as electrode material for ion-sensitive extended-gate FETs, IEEE Sens. J. 9 (2009) 277–284.
[16] W.T. Grubb, L.H. King, Palladium–palladium oxide pH electrodes, Anal. Chem. 52 (1980) 273–276.
[17] C.C. Liu, B.C. Bocchicchio, P.A. Overmyer, M.R. Neuman, A palladium–palladium oxide miniature pH electrode, Science 207 (1980) 188–189.
[18] E. Kinoshita, F. Ingman, G. Edwall, S. Glab, An examination of the palladium/palladium oxide system and its utility for pH-sensing electrodes, Electrochim. Acta 31 (1986) 29–38.
[19] L.J. Bloor, D.J. Malcolme-Lawes, An electrochemical preparation of palladium oxide pH sensors, J. Electroanal. Chem. 278 (1990) 161–173.
[20] V.A. Karagounis, C.-C. Liu, M.R. Neuman, L.T. Romankiw, P.A. Leary, J.J. Cuomo, Pd–PdO film potentiometric pH sensor, IEEE Trans Biom Eng BME-33 (1986) 113–116.
[21] M. Peuckert, XPS study on surface and bulk palladium oxide, its thermal stability, and a comparison with other noble metal oxides, J. Phys. Chem. 89 (1985) 2481–2486.
[22] N. Clément, K. Nishiguchi, J.F. Dufreche, D. Guerin, A. Fujiwara, D. Vuillaume, Water electrolysis and energy harvesting with zero-dimensional ion-sensitive field-effect transistors, Nano Lett. 13 (2013) 3903–3908.
[23] J. Go, P.R. Nair, B. Reddy, B. Dorvel, R. Bashir, M.A. Alam, Coupled heterogeneous nanowire-nanoplate planar transistor sensors for giant (>10 V/pH) nernst response, ACS Nano 6 (2012) 5972–5979.
[24] L.D. Burke, D.P. Whelan, A voltammetric investigation of the charge storage reactions of hydrous iridium oxide layers, J. Electroanal. Chem. Interfacial Electrochem. 162 (1984) 121–141.
[25] W. Olthuis, M.A.M. Robben, P. Bergveld, M. Bos, W.E. van der Linden, pH sensor properties of electrochemically grown iridium oxide, Sens. Actuators B: Chem. 2 (1990) 247–256.
[26] L. Bousse, S. Mostarshed, B. van der Schoot, N.F. de Rooij, Comparison of the hysteresis of Ta_2O_5 and Si_3N_4 pH-sensing insulators, Sens. Actuators B: Chem. 17 (1994) 157–164.
[27] S. Jamasb, S. Collins, R.L. Smith, A physical model for drift in pH ISFETs, Sens. Actuators B: Chem. 49 (1998) 146–155.
[28] W.D. Huang, H. Cao, S. Deb, M. Chiao, J.C. Chiao, A flexible pH sensor based on the iridium oxide sensing film, Sens. Actuators A: Phys. 169 (2011) 1–11.
[29] Y.-H. Liao, J.-C. Chou, Preparation and characteristics of ruthenium dioxide for pH array sensors with real-time measurement system, Sens. Actuators B: Chem. 128 (2008) 603–612.
[30] J.C. Chou, Y.F. Wang, Preparation and study on the drift and hysteresis properties of the tin oxide gate ISFET by the sol-gel method, Sens. Actuators B: Chem. 86 (2002) 58–62.
[31] J.L. Chiang, S.S. Jan, J.C. Chou, Y.C. Chen, Study on the temperature effect, hysteresis and drift of pH-ISFET devices based on amorphous tungsten oxide, Sens. Actuators B: Chem. 76 (2001) 624–628.

Biographies

Atanu Das received his B.S. and M.S. degrees in Physics from Vidyasagar University, India in 1999 and 2001 respectively. He received Ph.D. degree in Electronics Engineering from Chang Gung University, Taiwan in 2013. Currently, he is a post-doctoral researcher in Compound Semiconductor Research Group, Department of Electronic Engineering, Chang Gung University, Taiwan. His main research interests are GaN-based material growth in MOCVD, HEMT fabrication and characterization, high *k* for gate oxide and memory application, and electrochemical sensors.

Danny Hsu Ko received his B.S. degree in Chemical Science from University of Auckland, New Zealand in 2012. In 2013, he joined Professor Liann-Be Chang's research team in chemical sensor research. Currently, he is pursuing his M.S. degree in Department of Optoelectronics at Chang Gung University. His main research interests are nanomaterials, biosensor and optoelectronic devices.

Chia-Hsin Chen received his B.S. degree in Electronics Engineering from Chang Gung University, Taiwan in 2013. In 2013, he joined Professor Ray-Ming Lin's research group in GaN-based Device Research. Currently, he is pursuing his M.S. degree in Department of Electronics at Chang Gung University. His main research interest is fabrication of GaN-based MOS HEMT devices.

Liann-Be Chang received his B.S. degree from the Chiao-Tung University, Taiwan (1980) and the Ph.D. degree from the National Defense University, Taiwan (1987). Hence he was a post-doctoral fellow of the University of Illinois at Urbana-Champaign, U.S.A. in 1987–1988. He was a chief instrument engineer of Taiwan Power Co., Third nuclear power plant (1982–1984). He was also an associate professor, full professor and chairman of the Electronic Engineering Department, National Defense University (1998–2004). Later, he became a Chairman of the Electronic Engineering Department, Chang Gung University, 2004–2007. He is currently the vice Dean of College of Engineering and Director of the Green Technology Research Center, Chang Gung University. His multidisciplinary research interest includes the on design and fabrication of optoelectronic and microwave devices such as: PD, MSM, PIN, LED, MESFET, HEMT and III–V solar cells, SPR biosensors and compound semiconductor based EIS, EGFETs and LAPS devices.

Chao-Sung Lai received the B.S. and Ph.D. degrees from National Chiao Tung University, Hsinchu, Taiwan, in 1991 and 1996, respectively. In 1996, he joined the National Nano Device Laboratory, Hsinchu, Taiwan, where he has been engaged in the research of SOI devices. He won the Lam Award 1997. In 1997, he joined the Chang Gung University and Tao-Yuan, Taiwan, as an assistant professor, where he has been engaged in the research of the characterization and reliability of deep-submicron MOSFETs, nitrided thin gate oxides, shallow trench isolation and the modeling of dielectrics' reliability. He was the consultant of the Nan-Ya Technology Inc. for the 0.18 μm Logic-Team since 1997. In 2001, he visited the UC-Berkeley in the Department of Electrical Engineering for sabbatical research under Professor Chen Ming Hu in the Device Group. He was the consultant of the Nan-Ya Technology Inc. for the Flash Memory since 2001. He is the director of Bio-Sensor Group for Bio-Medical Research Center at Chang Gung University from 2007.

Fu-Chuan Chu received his B.S. degree from the Department of Electronics Engineering, Lee-Ming Institute of Technology, Taipei, Taiwan and M.S. degree from the Department of Electronics Engineering, Chung Cheng Institute of Technology, National Defense University, Taoyuan, Taiwan in 2007 and 2009, respectively. He received his Ph.D. degree in 2014 from Department of Electronic Engineering, Chang Gung University, Taoyuan, Taiwan. His research interests are epitaxy and fabrication of GaN-based HEMTs structure for RF applications.

Lee Chow is a professor at the Department of Physics, University of Central Florida, Orlando. He received his B.S. in Physics in 1972 from National Central University, Taiwan. He received Ph.D. in Physics from Clark University, Worcester, MA, USA in 1981. In 1981–1982, he was post-doc in Physics at the University of North Carolina, Chapel Hill, NC. He joined University of Central Florida in 1983 as an assistant professor, and was promoted to associate professor in 1988 and to professor in 1998. His areas of expertise include chemical bath deposition, nanofabrication of carbon nanotubes and metal oxides, diffusion in semiconductors, high T_C and diamond thin films.

Ray-Ming Lin received Ph.D. degrees in Electrical Engineering from National Taiwan University, Taiwan in 1997. During his Ph.D. work, he majored in the MBE growth and device application of metamorphic InGaAs/GaAs and InAlAs/GaAs buffer layers, quantum dot light emitting diode, room temperature infrared sensor. 1997–1999 he joined the Planning & Evaluation Division at National Science Council, Taiwan as an assistance research fellow. Since August 1999, he has been with the Department of Electronic Engineering of the Chang Gung University at Tao-Yuan, Taiwan where he is presently a full Professor. Since August 2001, Professor Lin has been the Director of Right and Technology Transfer Center at the Chang Gung University. His current research interests are in the areas of MOCVD technology development for the growth of nitride-based heterostructures, in situ fabrication of low-dislocation density, high-efficiency optoelectronic and high electron mobility transistor (HEMT) device structures and nano-biosensors.